

ters ($t_{1/2} = 66$ seconds and 110 minutes, respectively). Because of the short mean lifetimes of ^{17}F and ^{18}F , it is very unlikely that the (p,n) scheme could result in observable isotopic effects in O. We do not think that the large (up to 5 percent) isotopic O effects seen in certain carbonaceous chondrites (11, 12) can be explained in terms of the (p,n) scheme.

The case of Ne is more promising because solid objects in the solar system are very strongly fractionated in Ne; hence very small quantities of proton-produced stable Ne isotopes may be detectable. We have estimated the $R_{22/23} = (^{22}\text{Na}/^{23}\text{Na})_{\text{equilibrium}}$ ratios for the reaction $^{22}\text{Ne}(p,n)^{22}\text{Na}$ (^{22}Na , $t_{1/2} = 2.6$ years) in a gas of solar composition as $R_{22/23}^{-2.5} = 1.3 \times 10^{-10}$, $R_{22/23}^{-3.5} = 1.7 \times 10^{-11}$, and $R_{27/23}^{-4.5} = 2.4 \times 10^{-12}$. For the case of sudden condensation of Na, the quantities of ^{22}Ne that result from subsequent ^{22}Na decay in Na-containing solid phases are 7.4×10^{-9} , 5.6×10^{-9} , and $1.0 \times 10^{-8} \text{ cm}^3$ at standard temperature and pressure per milligram of Na for the three equilibrium ratios given above, which must be detectable in carbonaceous chondrites which typically contain 0.5 percent (by weight) of Na. Because of the short half-lives of ^{21}Na ($t_{1/2} = 23$ seconds) and ^{20}Na ($t_{1/2} = 0.4$ second), the $(^{21}\text{Na}/^{22}\text{Na})_{\text{equilibrium}}$ and $(^{20}\text{Na}/^{22}\text{Na})_{\text{equilibrium}}$ ratios in the gas are extremely low. We have considered all possible reactions in Na, Mg, Al, and Si that lead to ^{20}Na , ^{21}Na , and ^{22}Na and have concluded that neither of the two equilibrium ratios can be greater than 10^{-6} . Since the radioactive F-precursors ^{20}F , ^{21}F , and ^{22}F have half-lives of 11, 4.4, and 4 seconds, respectively, our scheme results in a Ne component that is virtually pure ^{22}Ne . Perhaps this is the origin of neon-E [for a discussion of neon E, see (13)].

The β^+ -emitting precursors of the stable Si isotopes have half-lives shorter than 2.5 minutes (^{30}P); hence we expect no isotopic anomalies in Si. The β^+ -emitting precursors of the stable S isotopes have half-lives shorter than 30 minutes (^{34m}Cl); hence we expect no isotopic anomalies in S.

The β^+ -emitting precursors of ^{36}Al and ^{38}Ar (^{40}Ar effects in solid objects are strongly masked by radiogenic ^{40}Ar from the decay of natural ^{40}K) have half-lives shorter than 7.7 minutes (^{38}K). Although Ar, like Ne, is strongly fractionated in solid objects, our preliminary estimates indicate that ^{38}Ar enhancements are probably undetectably small.

DIETER HEYMANN

MARLENE DZICZKANIEC

Department of Space Physics and
Astronomy and Department of Geology,
Rice University, Houston, Texas 77001

References and Notes

1. C. M. Gray and W. Compston, *Nature (Lond.)* **251**, 495 (1974).
2. T. Lee and D. Papanastassiou, *Geophys. Res. Lett.* **1**, 225 (1974).
3. S. P. Smith and J. C. Huneke, *Earth Planet. Sci. Lett.* **27**, 191 (1975).
4. M. Furukawa, K. Suizuri, K. Komura, K. Sakamoto, S. Tanaka, *Nucl. Phys. A* **174**, 539 (1971).
5. L. Aller, *The Abundance of the Elements* (Wiley-Interscience, New York, 1961).
6. R. C. Haymes, *Introduction to Space Science* (Wiley, New York, 1971).
7. W. A. Fowler, J. L. Greenstein, F. Hoyle, *Geophys. J. R. Astron. Soc.* **6**, 148 (1962).
8. L. V. Kuhl, *Astrophys. J.* **140**, 1409 (1964).
9. G. H. Herbig, *Spectroscopic Astrophysics* (Univ. of California Press, Berkeley, 1970).
10. L. Grossman, *Geochim. Cosmochim. Acta* **36**, 597 (1972).
11. R. N. Clayton, L. Grossman, T. K. Mayeda, *Science* **182**, 485 (1973).
12. ———, N. Onuma, in *Proceedings of the Soviet-American Conference on the Cosmochemistry of the Moon and Planets*, N. J. Hubbard and J. H. Pomeroy, Eds. (U.S.S.R. Academy of Sciences, Moscow, in press).
13. D. C. Black, *Geochim. Cosmochim. Acta* **36**, 377 (1972).
14. I thank Dr. D. D. Clayton for stimulating discussions, Dr. Huneke for allowing me to quote from his unpublished paper, and the two unknown reviewers for their constructive criticism. This research was supported by NASA grant NGL-44-006-127.

11 July 1975; revised 2 September 1975

Laboratory Simulation of Thermal Convection in Rotating Planets and Stars

Abstract. *Because of dynamical constraints in a rotating system, the component of gravity perpendicular to the axis of rotation is the dominant driving force of convection in liquid planetary cores and in stars. Except for the sign, the centrifugal force closely resembles the perpendicular component of gravity. Convection processes in stars and planets can therefore be modeled in laboratory experiments by using the centrifugal force with a reversed temperature gradient.*

Convection driven by thermal buoyancy is a major source of fluid motions in planets and in stars. In general, buoyancy forces result from superadiabatic temperature gradients in the nearly spherically symmetric gravity fields of celestial bodies. Progress in the understanding of natural convection processes has depended to a large extent on the interaction of theoretical analysis and experimental observation (1). Because of the difficulty of simulating spherical gravity in the laboratory, experimental investigations have been restricted to convection in a plane layer heated from below. Both this case and convection in a spherical fluid shell of a nonrotating planet or star share the property of horizontal isotropy. When rotation becomes important the spherical symmetry is lost and the analogy with the laboratory convection layer no longer holds. The most significant difference arises from the fact that the angle between gravity and the vector Ω of angular velocity varies in self-gravitating bodies, while the two vectors must be parallel in the laboratory experiment. When Ω is inclined with respect to the vertical, gravity gives rise to a nonstationary body force in the rotating system. Although it may appear that the experimental simulation of convection in rotating self-gravitating spherical systems is even more difficult than in the nonrotating case, the presence of the centrifugal force in a rotating laboratory apparatus provides a new possibility for simulation experiments, as we outline in this report.

The importance of rotation for the dynamics of fluids is measured by two non-dimensional parameters, the Ekman num-

ber and the Rossby number. The latter represents the ratio between the vorticity of motions relative to the rotating system and the angular velocity Ω . The Ekman number is defined by

$$E = \nu/L^2\Omega$$

where ν is the kinematic viscosity of the fluid and L is a typical length, say the radius of a planetary liquid core. In many applications both the Ekman and the Rossby number are very small. In the limit where these parameters vanish the Proudman-Taylor theorem for a stationary velocity field \mathbf{v} in a homogeneous incompressible fluid holds

$$\Omega \cdot \nabla \mathbf{v} = 0 \quad (1)$$

This equation states that the velocity cannot vary in the direction of the axis of rotation. The theorem also holds for a barotropic fluid if the velocity vector is replaced by the momentum vector.

Motions with a nonvanishing radial component in a fluid sphere or spherical shell cannot satisfy Eq. 1 exactly because the normal velocity component must vanish at the boundary. On the other hand, strongly time-dependent flows, which do not have to obey Eq. 1, are inefficient in releasing potential energy because of the phase lag between thermal buoyancy and radial motion. The theoretical investigation (2) of the problem shows that in the realized convective flow the constraint of Eq. 1 is overcome by the combination of a slow time dependence and viscous forces associated with the small length scale in the azimuthal direction. As shown in Fig. 1, the motions occur in the form of thin

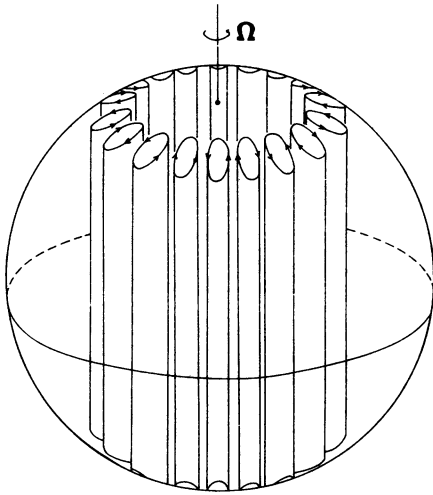
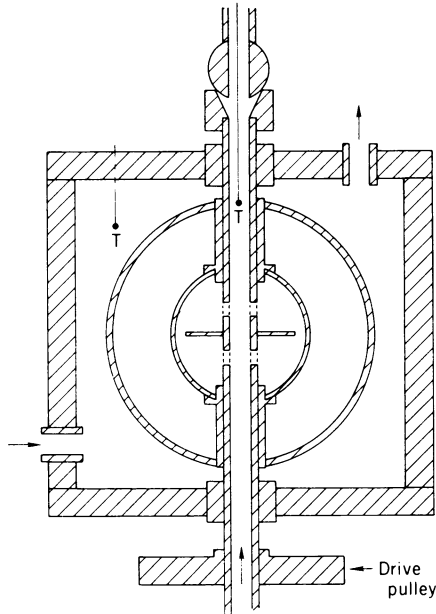


Fig. 1 (left). Qualitative sketch of convective motions in a rotating, self-gravitating fluid sphere. Fig. 2 (right). Schematic diagram of experimental apparatus; T denotes thermocouple.



columns parallel to the axis of rotation, which propagate slowly in the eastward direction. It is evident from the form of the motions that in the first approximation, only the component of gravity perpendicular to the axis of rotation provides the driving force. This is the key to the laboratory simulation experiment.

The fact that the convective motion depends little on the component of the buoyancy force parallel to Ω minimizes the influence of gravity in a convection experi-

ment rotating about a vertical axis. The centrifugal force is identical in its spatial dependence to the component of gravity perpendicular to the axis of rotation in a homogeneous self-gravitating fluid sphere. Thus, it is well suited to simulate the buoyancy force in celestial bodies. To compensate for the difference in the sign of the forces, the temperature gradient must be reversed in the laboratory experiment. Since only the product of temperature gradient and gravity enters the equations of

convection, the reversal does not affect the dynamics of the system within the Boussinesq approximation, which assumes a constant density except in the gravity term.

A sketch of the laboratory apparatus is shown in Fig. 2. Two concentric spheres, the outer one made of transparent material (Plexiglas or Lucite), are fixed to a vertical shaft, which functions as the axis of rotation. The spherical layer between the spheres is filled with water to which small flaky particles (3) have been added to aid visualization. Cold water from a thermostatically controlled bath of temperature T_1 flows through the rotating shaft to keep the inside of the inner sphere at a constant temperature. The system is immersed in a rectangular box of transparent plastic material through which water of constant temperature T_2 is circulating. When T_2 exceeds T_1 and a sufficiently high rotation rate is used, a highly nonaxisymmetric state of convection sets in. The convection columns are regularly spaced, reflecting closely the theoretically calculated solution, as shown in Fig. 1 for a slightly different temperature distribution. When the rotation rate is increased further, convection columns tend to fill the outer part of the annulus, as shown in Fig. 3. Because of differences in the phase velocity of azimuthal propagation, the columns become irregularly spaced while retaining their perfect alignment with the axis of rotation.

In the case of Fig. 3 the ratio between

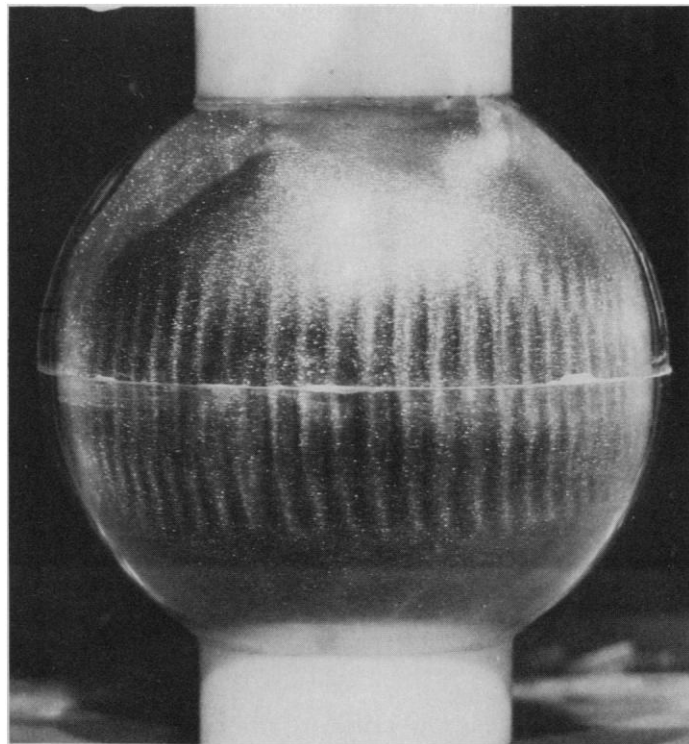
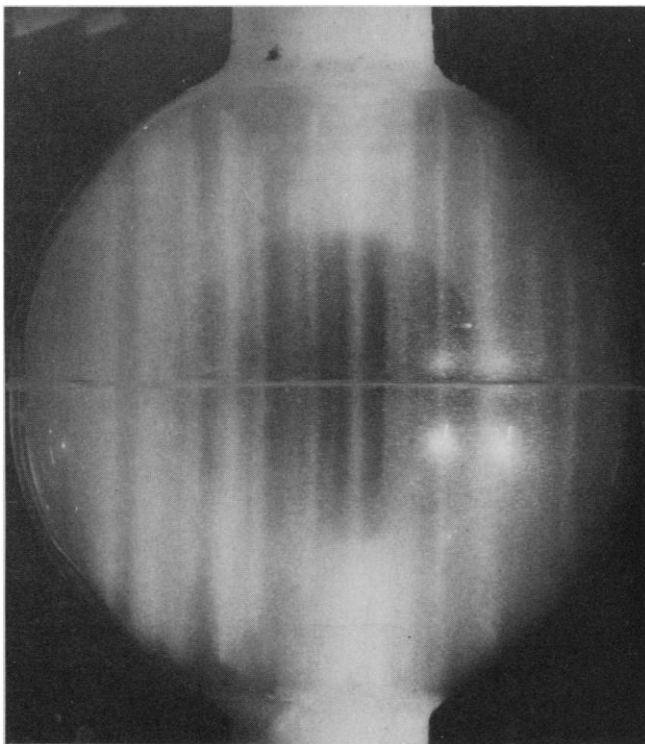


Fig. 3 (left). Convection columns in a rotating spherical shell heated from the outside and cooled from within. The flow is visualized with small flaky particles which become oriented with the shear. Fig. 4 (right). Convection in a thin rotating spherical shell heated from within. The banana-shaped convection cells are made visible by small neutrally buoyant particles aligned with the direction of shear. The gap width is approximately $1/16$ of the radius.

the inner and outer radii of the fluid shell is approximately $\frac{1}{2}$. This case simulates convection in the liquid core of the earth when magnetic effects can be neglected. If convective motions do occur in the earth's core it is likely that they generate the earth's magnetic field (4). Although the Lorentz forces are dynamically important, it is necessary to investigate the non-magnetic case in order to understand the origin of the geomagnetic field. The laboratory experiment is well suited for this purpose since it allows for the study of aspects of the problem which are not easily accessible to theoretical analysis, such as a differential rotation caused by the non-linear interaction of the convection columns.

Figure 4 shows convection in a thin shell. The small thickness of the fluid layer permits the realization of a relatively high Ekman number without lowering the rotation speed of the apparatus below a value of approximately 60 rev/min, where effects of gravity become noticeable. The experiment demonstrates a convection pattern which was proposed in connection with a new theory of the solar differential rotation (5). By parameterizing the effects of small-scale motions in the solar atmosphere in terms of an eddy viscosity, it was shown that giant convection cells (6) of a form similar to that shown in Fig. 4 give rise to a differential rotation which agrees in all qualitative aspects with that observed on the sun. Although neither theory nor experiment is capable of simulating the detailed structure of solar convection, the strong north-south correlation of large-scale convection is borne out by the phenomenon of "active longitudes" and the north-south coherence of solar magnetic fields (7).

Measurements of the onset of convection as a function of rotation rate and temperature difference have been compared with the results of linear theory and will be published separately (8). The good agreement with the theoretical predictions indicates that this relatively simple experiment can be valuable for exploring and understanding the large variety of non-linear processes which confront scientists studying the dynamics of convection in rotating planets and stars.

F. H. BUSSE
C. R. CARRIGAN

Department of Geophysics and
Space Physics, University of
California, Los Angeles 90024

References and Notes

1. An introduction to the linear theory of convection is given by S. Chandrasekhar, *Hydrodynamic and Hydromagnetic Stability* (Clarendon, Oxford, 1961).
2. F. H. Busse, *J. Fluid Mech.* **44**, 441 (1970).
3. Solution AQ 1000, Kalliroscope Corp., Cambridge, Mass.

4. E. C. Bullard, *Proc. R. Soc. Lond. Ser. A* **197**, 433 (1949); F. H. Busse, *Geophys. J. R. Astron. Soc.* **42**, 437 (1975).
5. F. H. Busse, *Astrophys. J.* **159**, 629 (1970).
6. V. Bumba, R. F. Howard, S. F. Smith, in "Annual report of the director, Mount Wilson and Palomar Observatories (1963-1964)"; V. Bumba, in *Proceedings of the International School of Physics "Enrico Fermi,"* P. A. Sturrock, Ed. (Academic Press, New York, 1967), course 34.
7. F. H. Busse, *Astron. Astrophys.* **28**, 27 (1973).
8. ——— and C. R. Carrigan, in preparation.

- 11 August 1975

Activity of Nocturnal Primates: Influences of Twilight Zeitgebers and Weather

Abstract. *The time of onset of activity of bush babies (Galago senegalensis), slow lorises (Nycticebus coucang), and an owl monkey (Aotus trivirgatus) living in outdoor enclosures usually fell in certain illuminance ranges of dusk and kept pace with seasonal progressions of sunset time. Influences of cloud cover were variable, but excessive heat and cold were inhibitory. Accurate endogenous timekeeping and reliance on the most stable zeitgeber apparently maintain activities in synchrony with the rhythmically changing environment.*

Under natural conditions, activity rhythms usually become synchronized with (entrained to) the earth's rotational period as a result of responses to certain periodic environmental changes, or zeitgebers, of which illuminance is often the most important. For many animals the photic zeitgebers are believed to involve the twilight periods. Many animals customarily begin or cease activity during twilights (1-3), and simulated twilights influence the activity of numerous captive mammals (4-8).

It is virtually impossible to determine the isolated influences of twilights through field studies [but see (3)] because of the confounding influences of environmental variables, such as cloud cover, temperature, and food availability. The behavioral inconstancy during twilights may obscure functional relationships that only emerge when the naturalist's findings are complemented with results of controlled studies.

We are studying small and medium-sized mammals by monitoring locomotor activity in outdoor and indoor activity-wheel enclosures (7, 9). Natural light and weather are the primary variables outdoors, while the chief indoor variable is a cyclic light regime with artificial twilights. We report here briefly our outdoor findings for the activity onset and cessation times of seven individuals belonging to three species of nocturnal primates [see (8) for detailed results]. The ability of the animals to maintain entrainment in variable weather confirms certain a priori expectations about the role of twilights in modulating the endogenous physiological clock. We suggest a new role for the duplex retina as a physiological relay between twilight light changes and the endogenous clock.

Our animals included three African lesser bush babies (*Galago senegalensis*), three Asian slow lorises (*Nycticebus coucang*), and one male South American owl mon-

key (*Aotus trivirgatus*). All were mature, wild-caught, and fed as described (6). Two enclosures were used. The "roof" enclosure (10) was our primary data collecting system. It was located above a penthouse on the roof of the Life Sciences Building at the University of California, Los Angeles, and consisted of an activity wheel 122 cm in diameter adjoining a wire-mesh cage with a heated nest retreat. It was housed in a wire-mesh cubical, to the top and sides of which were fastened artificial plants in a very dense arrangement, giving both heavy cover and a seminatural setting.

The "run" enclosure was located nearby but 4 m lower. It contained an activity wheel and a sheltered nest retreat. The wheel in the run received only indirect light when the sun was low on the horizon, and it was more sheltered from both wind and rain than that on the roof. Thirty minutes before sunset the illuminance (all values measured at the bottom of the wheel) in the run was only 15 percent of that in the roof wheel; at sunset it was 44 percent. By 10 minutes after sunset the illuminances were equal.

All individuals adapted to locomotion in wheels as an activity outlet within a few days. Systems controls, monitoring, and data reduction methods have been described (4, 11). Digital printers and strip-chart recorders gave the times of initiation, duration, and cessation of activity (wheel revolutions) and half-hourly totals for wheel revolutions in both enclosures. Strip-chart analog records gave the time and instantaneous speed and direction of running in the roof enclosure; we also obtained half-hourly printouts of time spent running. Meteorological variables were recorded simultaneously (7) on the analog records from the roof enclosure.

All animals were almost strictly nocturnal [night plus twilights (12), Table 1]. An animal usually entered the wheel during dusk and became sustainedly active at